Numerical Study of the Cone Angle Effect on Conical Basin Gravitational Water Vortex Turbine

Sugianto[1] Haryadi[1,*] Prasetyo[1]

[1] *Mechanical Engineering Department, Politeknik Negeri Bandung*
[*] *Corresponding author. Email: haryadi.mesin@polban.ac.id*

ABSTRACT
Free vortex almost always occurs in open streams. The Gravitational Water Vortex Turbine (GWVT) is expected to extract energy from this phenomenon. The turbines are expected to be at the forefront of harnessing the potential of low hydro head energy. However, this effort needs to describe fluid motion in a vortex field, of course, which is very difficult. For the purpose of preliminary calculations for the GWVT design, a simple equation to calculate the vortex strength in a cylindrical vortex basin is available. Some researchers suggest using a conical basin. Therefore the flow pattern in the vortex field can no longer be predicted using these simple equations. The cone angle should be optimized. In this study, a performance comparison of conical basin GWVT with three variations of the conical angle, namely 15º, 20°, and 25º, was carried out. The runner used in this study was in the form of a conical Savonius Wind Turbine Blade (SWTB) with equal taper angles, which have 5 blades. Each blade is a segment of a cylinder, with a segment angle of 120º or one-third of the cylinder to form a 60º inlet angle. Rotary speed was selected at 60 rpm. The runner taper angle was equal to the cone angle of the basin. The runner sweep area for the three variations of the tapper angle was equal to maintain fair comparison. The method used to perform this comparison was CFD simulation because the vortex equations were no longer valid for the conical basins. The software used was ANSYS Fluent. Meanwhile, the solver used was steady-state 3D, pressure-based. The turbulence model used was SST k-ω for the area near the wall and free stream area. For meshing, the hexagonal form was used for all computation domains. The MRF (Multiple Reference Frame) technique was used for fluid flow near rotating blades. It was concluded, from this study, that the conical basin with a 15° cone angle gave the highest torque and shaft power.

Keywords: *Cone angle, Savonius, Vortex, Turbine.*

1. INTRODUCTION

Free Vortex almost always occurs in open streams, which can be utilized to produce mechanical power. The vortex water gravitational turbine (GWVT) is expected to be able to extract energy from this phenomenon. However, this effort needs to describe fluid motion in a vortex field, of course, which is very difficult. For the purpose of preliminary calculations for the GWVT design, a simple equation to calculate the vortex strength in a cylindrical vortex basin is available, as shown by Equation (1) [1]. The equation was taken from the Rankine vortex model [2]. In addition to the Rankine model, there is the Odgard model and several other models. The model proposed by Azarpira-Zarati provides formulas for calculating tangential velocity and radial velocity [3].

$$v_\theta = \frac{K}{2 \times \pi \times r} \quad (1)$$

$$K = \frac{Q}{h} \quad (2)$$

2. BACKGROUND

GWVT's main components are an open channel, vortex basin, and runner. The vortex basins were usually cylindrical in shape. In recent years, some researchers have suggested using conical basins [4, 5]. Thus the flow pattern in the vortex field can no longer be predicted using these simple equations. With the runner in the vortex field, the flow pattern becomes even more complex. Numerical methods, however, are still reliable for predicting the flow pattern and the effect of fluid flow on runners.

Wanchat et al. performed simulations using ANSYS Fluent [6], Dhakal et.al.[4], and Shabara et.al.[7], performed calculations on vortex pools and runners using CFD (Computational Fluid Dynamics).

Nishi and Inagaki conducted a GWVT study by comparing simulations and experiments. The turbine runner is radial, while the vortex pool is cylindrical. Simulations were carried out using ANSYS CFX15.0 software. The method used is Volume of Fluid, 2 phases, with water and air as working fluids. The basin and runner sections are divided into about 446.00 and 541.00 cells respectively, while the upstream and downstream parts are about 434,000 and 780.00 cells. The simulation begins with steady conditions and continues with transients. From these transient simulations, the water surface profile was obtained. The performance shown by the simulation results is close to the experimental results. The highest efficiency occurs at 122 rpm, with an efficiency of 35.4% [8].

Various options in CFD simulation for conical basin GWVT are ranging from the software used to the flow model used. The transient model can be used to obtain results that are closest to reality, 2-phase water and air, MM (Moving Mesh), MM (Moving Mesh). Completion with this method requires a very large computational capacity.

The next option is to use a single-phase, steady-state model, incompressible. Tonello et al. carried out a steady-state 3D Francis-99 Tokke Turbine simulation [9]. Bajracharya et al. researched to determine the effect of various geometric parameters on the GWVT conical runner. The blade runner is in 2D shape. In this study, 7 sets of runner shapes were investigated. The simulation was carried out with ANSYS Fluent, steady-state 3D, pressure-based, MRF (Multiple Reference Frame) concepts. The fluid is assumed to be a single-phase with a flat surface. In this way, computations can be done quickly and give results that are close to experiments [5]. This option requires much less computational capacity but gives good results.

3. RESEARCH METHODS

The previous study shows that the performance of GWVT with conical basin provides better performance than those of cylindrical one, but the tapper angle should be optimized. In this study, a comparison of the performance of the conical basin GWVT with three variations of the conical angle, namely 15º 20 and 25º, will be carried out. The runner that will be used in this study is in the form of the Savonius Wind Turbine Blade (SWTB), which consists of 5 blades and for next called Gravitational Water Vortex – Savoius Turbine (GWVST). Each blade is a segment of a cylinder, with a segment angle of 120º

For simplicity, the simulation was carried out in this study with a single water phase and assumed as a steady flow or one-third of the cylinder to form a 60º inlet angle. Rotary speed is selected at 60 rpm. To get a fair comparison, the runner sweep area for the three variations of the tapper angle is equal. The method used to perform this comparison is CFD simulation. The software used was ANSYS Fluent. Meanwhile, the solver used was Steady-state 3D, pressure-based. The turbulence model used was SST k-ω. Hexagonal grid for all of the domain computation. Open channels were treated as closed flows with slopes. The free surface was modeled as a pressure out.

So far, between 15º - 25º, the tapper angle area was considered the most likely to be varied. Less than 15º can be considered less conical so that it resembled a cylinder and required a head that was too large, while at a tapper angle of 25º, the radius of the bottom of the runner was too small.

The clearance distance between the runner and the basin wall was also kept constant at 0.06 m. The upper radius of the blade was 175 mm, with a blade thickness of 3 mm. The angle of entry was 60º. The swap area was kept constant, at 0.0315 m2. For this reason, the blade heights were 0.216 m, 0.256 m, and 0.297 m, respectively.

Based on equations (1) and (2), the v_θ value depends on the value of K only with the simulation conditions carried out at the value of Q and h was constant. So the value of K only depends on the geometric shape of the GWVST, which was identified as Savonius runner. The value of K or v_θ can be obtained through a numerical simulation process of water flow that interacts with the runner and basin. The approach was taken to obtain the value of K or v_θ to use the MRF model in the numerical simulation process as described in Figure 1. The coordinate system of the linear translational $\vec{v}_t$ and rotational velocity $\vec{\omega}$ moved relative to a stationary reference coordinate. The coordinate origin of the moving system was positioned with a vector $\vec{r}_0$ with respect to the origin of the stationary coordinate. The rotation axis is defined as the direction of the unit vector $\hat{a}$ so that it can be written as $\vec{\omega} = \omega\hat{a}$:

The MRF computational space for the numerical simulation process refers to a moving coordinate system. Therefore any point in the MRF space is positioned as a position vector $\vec{r}$. The velocity of the water can be transformed from a stationary coordinate system to a moving coordinate system using the following equation [10]

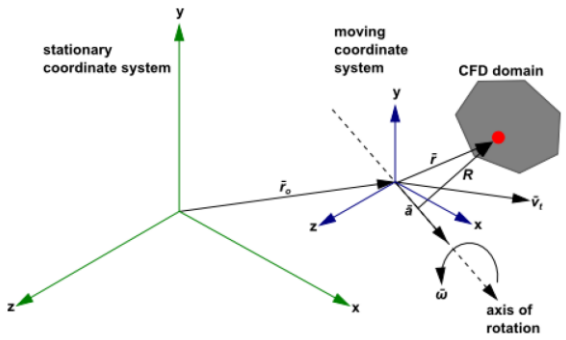

Figure 1. Stationary and Moving Reference Frame [10]

$$\vec{u}_r = \vec{v}_t + \vec{\omega} \times \vec{r} \quad (4)$$

$$\vec{v}_r = \vec{v} - \vec{u}_r = \vec{v}_t + \vec{\omega} \times \vec{r} \quad (5)$$

$\vec{v}_r$ is the relative velocity (velocity as seen from the moving coordinates). $\vec{v}$ is the absolute velocity (velocity seen from the stationary coordinates). $\vec{u}_r$ is the velocity of the moving coordinates which is moving relative to the inertial coordinates. $\vec{v}_t$ is the translational velocity of the coordinates, and the rotational speed.

The fluid motion equation (transport equation) at steady and incompressible conditions (ANSYS Fluent's pressure-based solvers) can be solved in the MRF by entering $\vec{v}_r$ and $\vec{v}$ into the mass conservation equation, Equation 6, and the momentum conservation equation, Equation 7[10] that is

$$\nabla \cdot \vec{v}_r = 0 \quad (6)$$

$$\rho \nabla \cdot (\vec{v}_r \vec{v}) + \rho \left[\vec{\omega} \times (\vec{v} - \vec{v}_t) \right] = -\nabla p + \nabla \cdot \bar{\tau} + \rho \vec{g} + \vec{F} \quad (7)$$

Where $\left[\vec{\omega} \times (\vec{v} - \vec{v}_t) \right]$ is Coriolis and centripetal acceleration, p is static pressure, $\rho \vec{g}$ is the gravitational force, $\vec{F}$ is external force, and $\bar{\tau}$ stress tensor, Equation 8, [10] that is:

$$\bar{\tau} = \mu \left[\left(\nabla \vec{v} + \nabla \vec{v}^T \right) - \tfrac{2}{3} \nabla \vec{v} I \right] \quad (8)$$

Where μ is molecular viscosity and I is unit tensor.

It is understood that all variables of fluid flow properties listed in Equations 4,5,6,7,8 as a function of space and time, and in general, it can be expressed in terms of the main fluid properties, namely mass density $\rho(x, y, z, t)$, stress $p(x, y, z, t)$, temperature $T(x, y, z, t)$, and velocity vector $\vec{u}(x, y, z, t)$. If all the variables of the flow properties are written in the form of a general variable, then the form of conservation of mass, momentum, and energy in steady conditions can be written in the form of a single equation known as the transport equation for the variable properties, ϕ (Equation (9)) [11].

$$\nabla (\rho \phi \vec{u}) = \nabla (\Gamma \text{grad} \phi) + S_\phi \quad (9)$$

Equation (9) for the numerical simulation process using the control volume CFD method can be written in integral form as [11]

$$\int_{CV} \nabla (\rho \phi \vec{u}) dV = \int_{CV} \nabla (\Gamma \text{grad} \phi) dV + \int_{CV} S_\phi dV \quad (10)$$

The first step to obtaining a numerical solution ϕ of equation (10) was the process of making the geometry of the GWVST computational space. The computational space consists of an open channel, a conical basin with a conical runner inside. The cone angle of the conical basins was varied into 15º, 20º, and 25º. The conical runners utilize 5 Savonius blades, and have equal taper angle with the cone angle of the basin, as shown in Figure 2.

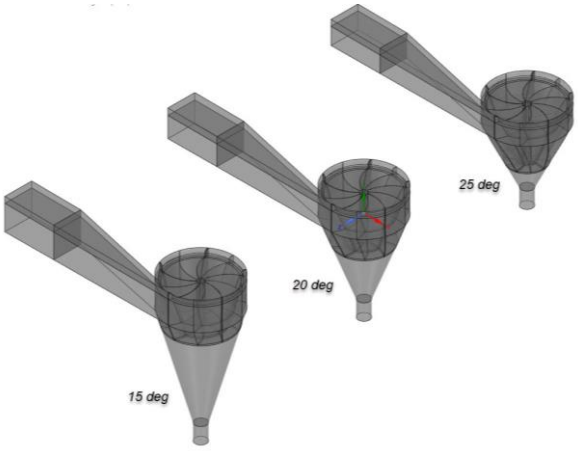

Figure 2. GWVST geometry

The GWVST geometry mesh development was carried out using a block meshing system. The block mash consists of channel block mesh, conic block mesh, drain block mesh, and runner block mesh as shown in Figure 3.

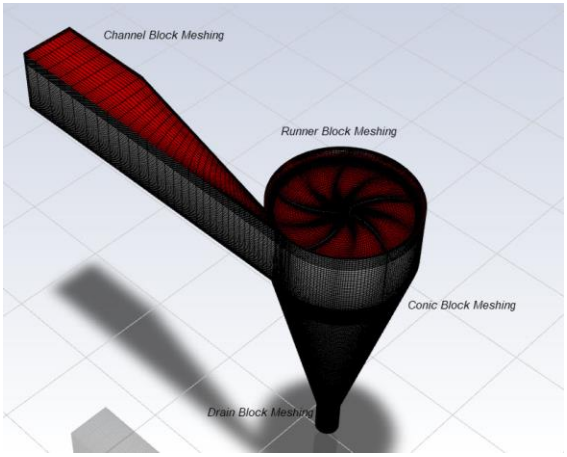

Figure 3. GWVST meshing process using a block mesh system (as sample 20 deg)

In particular, the runner block mesh was treated as a rotating fluid using the Multiple Reference Frame (MRF) model. The number of mesh cells for all of the mesh blocks is described in Table 1.

Table 1. The number of meshing cells

Tapper angle	Hexahedra Element type of Block Mesh				
[degree]	Channel	Runner	Conic	Drain	Total Number
15	28800	546636	1832985	289180	2697601
20	28800	546476	1352558	288380	2216214
25	28800	546762	996016	289760	1861328

The boundary conditions of the numerical simulation process of water flow in the GWVST computational domain are: the water volumetric flow rate was 6 liters/s, the turbulent flow model was SST k-ω, and the air-water contact interface pressure was 1 atm (open channel model approach).

4. CONCLUSION

The fluid velocity distribution resulted from the simulation process for the three tapper angle in a certain (constant) field of vortex flow strength is shown in Figure 4. It can be seen in Figure 4 that the whirl near the rotating runner is represented by a tangential velocity distribution (velocity curl Y) on the three XZ section planes, as shown in Figure 5.

It can be seen from the bottom of the runner towards the drain in Figure 5 that the tangential velocity increases towards the drain hole. The increase in tangential velocity at the cone angle of 15 is relatively higher than the taper angle of 20 and 25 degrees. The tangential velocity increase can be more clearly seen in the distribution of tangential velocity in the XY plane section, as shown in Figure 6.

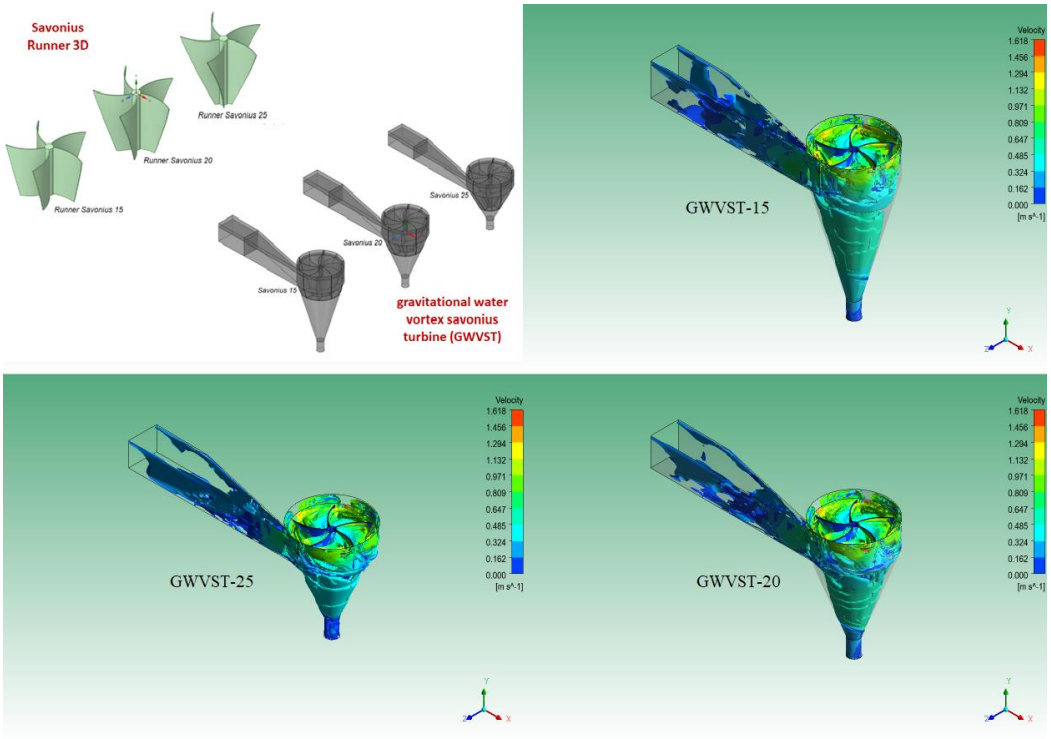

Figure 4. Distribution of water flow velocity on a plane that has a constant whirlpool strength

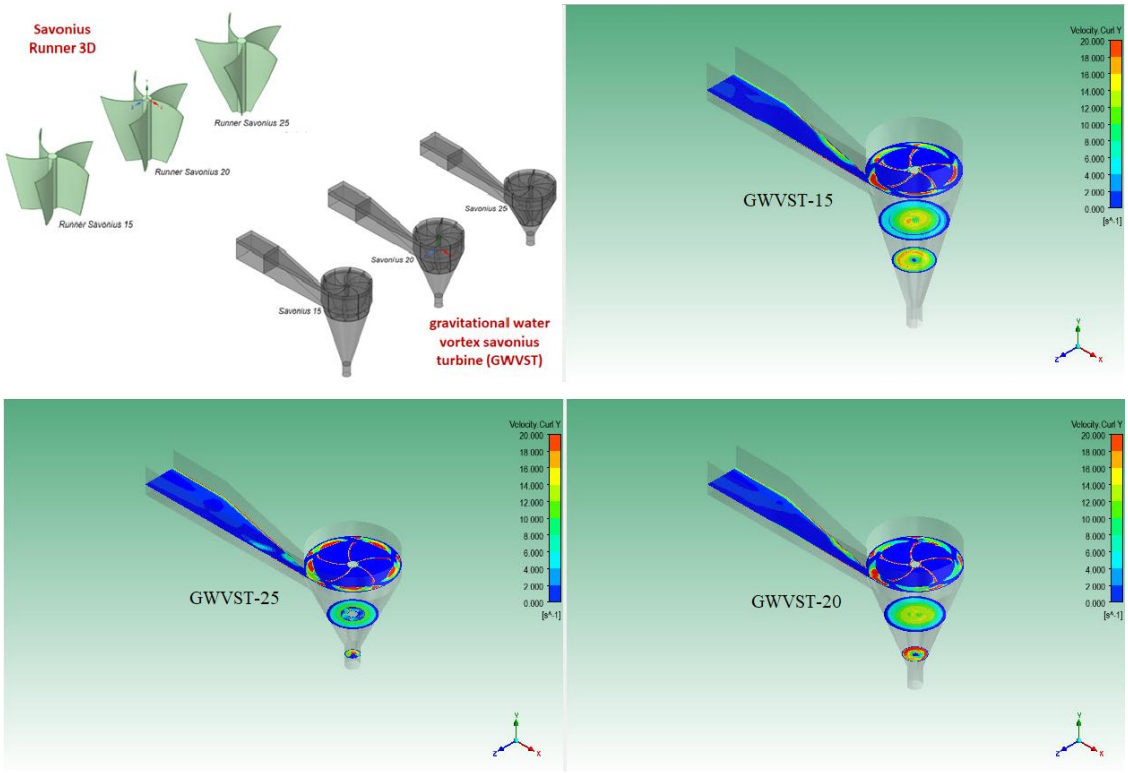

Figure 5. Distribution of tangential velocity on XZ plane

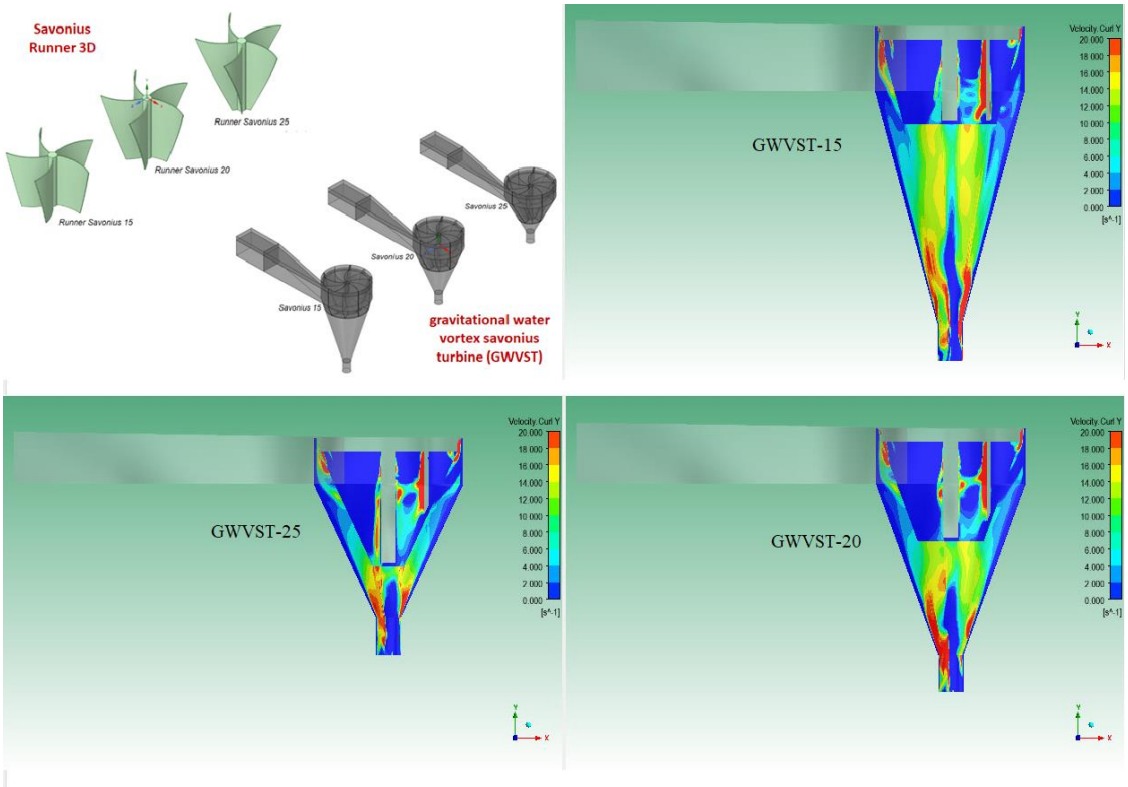

Figure 6. Distribution of tangential velocity on the XY section plane

It can be seen in Figure 6, at the area between the bottom of the runner and the drain hole that tangential velocity increase as the flow flows close the drain hole. The tangential velocity increase is relatively higher at the tapper angle of 15 than the taper angle of 20 and 25 degrees. This tangential velocity increase causes an increase in turbulence kinetic energy towards the center of the basin axis, as shown in Figure 7.

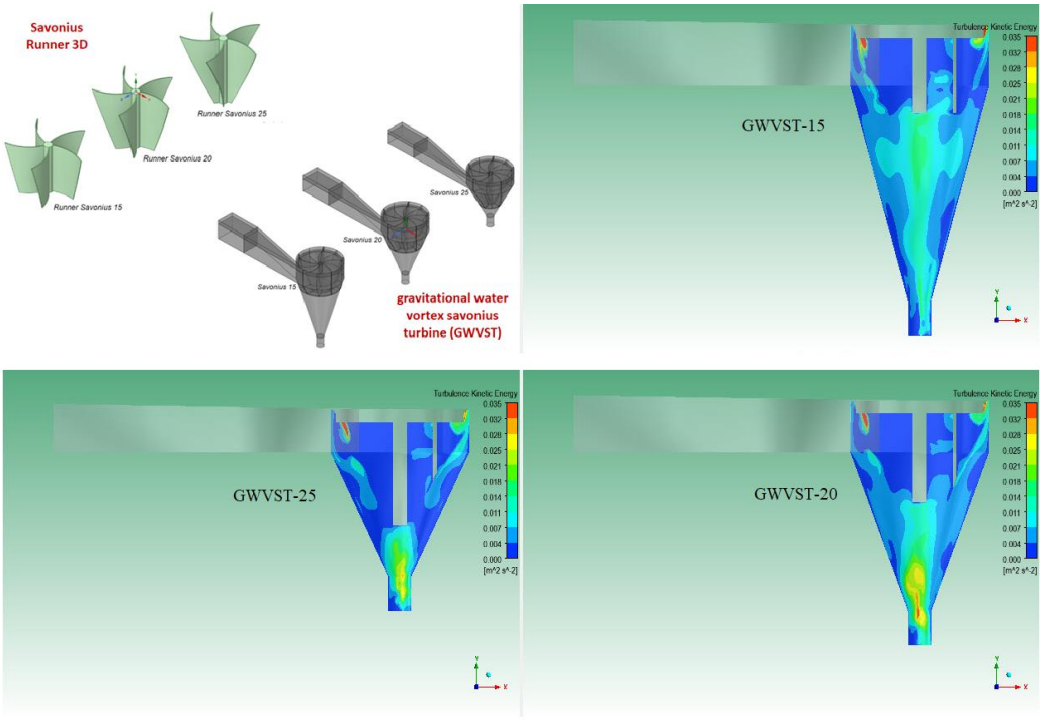

Figure 7. Distribution of turbulence kinetics energy on the XY section plane

Based on Figure 7, the distribution of turbulence kinetic energy has increased towards the basin axis or the axis of runner rotation. The increase in turbulent kinetic energy of water flow in the basin towards the drain can be more clearly, as shown by a curve in Figure 8.

It can be seen in Figure 8 that the turbulence kinetic energy is relatively higher along the radial line as a result of an increase in the tangential velocity (Figure 9) which is relatively higher at the tapper angle of 15° compared to the angle of 20º and 25º.

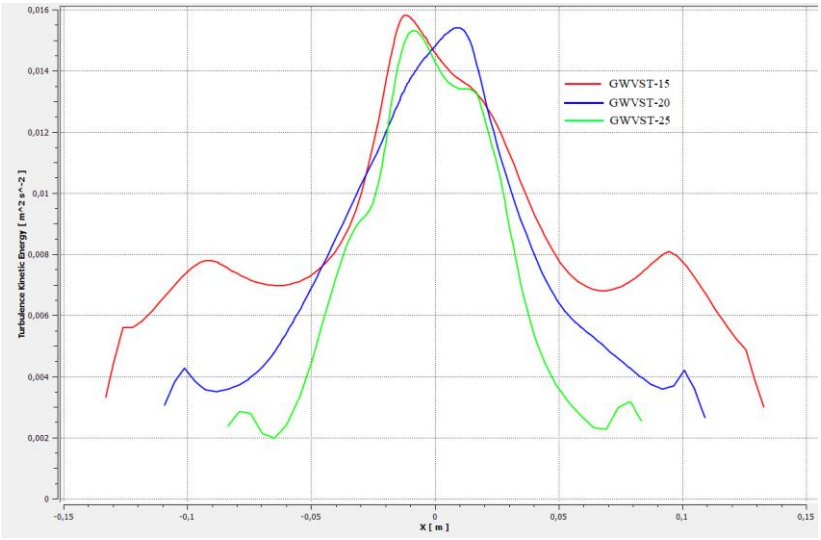

Figure 8. Kinetic energy curve of the water flow turbulence toward the rotation axis along the radial line

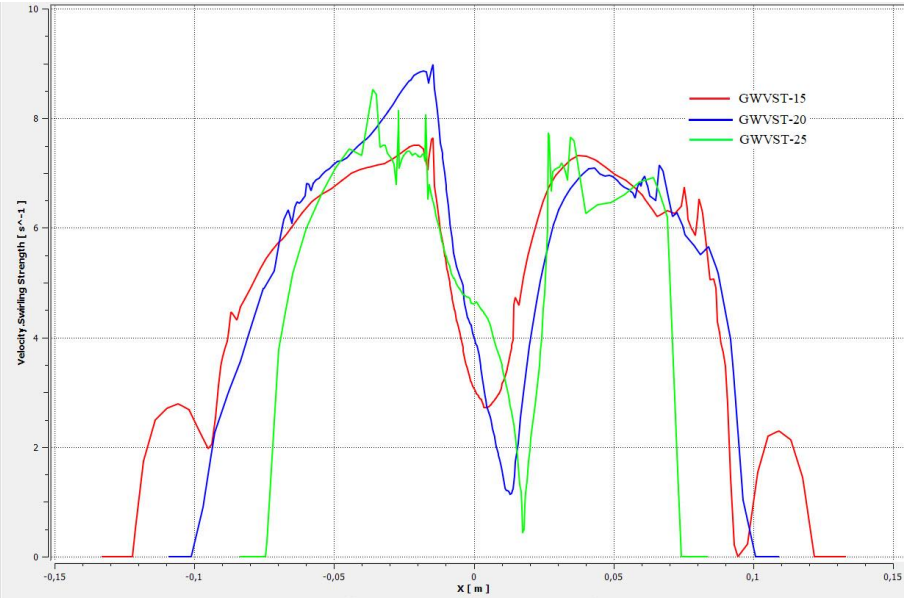

Figure 9. Vortex strength along radial lines

Based on the simulation results in Figures 4 to 9, it is clear that the farther the drain position from the lower runner is identified by the smaller the cone angle. The smaller the backflow is towards the runner so that the water flow resistance is smaller, which has the potential to increase the torque generated by the runner. This can be shown by the tangential velocity distribution as shown by the tangential velocity curve to the basin radius as shown in Figure 9 above, so that the power generated will be greater with the smaller the tapper angle, as shown in Table 2.

Table 2. Torque and power exerted by the GWVT

Tapper angle	Volumetric flow rate	Angular velocity of runner		Torsion	Power
[degree]	[liters/s]	[rpm]	[rad/s]	[N.m]	[watt]
15	6	60	6,28	2,33	14,61
20	6	60	6,28	1,95	12,25
25	6	60	6,28	1,65	10,32

ACKNOWLEDGMENT

This research was funded with PPDS - KBK Loan No.: B/78.4/PL1.R7/PG.00.03/2001, Politeknik Negeri Bandung.

REFERENCES

[1] T. R. Bajracharya, Development and Testing of Runner and Conical Basin for Gravitational Water Vortex Power Plant, vol. 10, no. 1. Lalitpur: Centre for Energy Studies (CES) Institute of Engineering, Tribhuvan University, Nepal, 2014.

[2] F. M. White, Fluid Mechanics, (2003), 4th ed. Boston: WCB McGraw-Hill., 1998

[3] M. Azarpira and A. R. Zarrati, “A 3D analytical model for vortex velocity field based on spiral streamline pattern,” Water Sci. Eng., vol. 12, no. 3, pp. 244–252, 2019.

[4] S. Dhakal et al., “Comparison of cylindrical and conical basins with an optimum position of runner: Gravitational water vortex power plant,” Renew. Sustain. Energy Rev., vol. 48, no. August, pp. 662–669, 2015.

[5] T. R. Bajracharya et al., “Effects of Geometrical Parameters in Gravitational Water Vortex Turbines with Conical Basin,” J. Renew. Energy, vol. 2020, no. Figure 1, pp. 1–16, 2020.

[6] S. Wanchat, R. Suntivarakorn, S. Wanchat, K. Tonmit, and P. Kayanyiem, “A parametric study of a gravitation vortex power plant,” Adv. Mater. Res., vol. 805–806, no. May, pp. 811–817, 2013

[7] H. M. Shabara, O. B. Yaakob, and Y. M. Ahmed, “CFD Validation for Efficient Gravitational Vortex Pool System,” J. Teknol., vol. 5, no. May, pp. 97–100, 2015

[8] Y. Nishi and T. Inagaki, “Performance and Flow Field of a Gravitation Vortex Type Water Turbine,” Int. J. Rotating Mach., vol. 2017, pp. 1–11, 2017.

[9] N. Tonello, Y. Eude, B. de L. de Meux, and M. Ferrand, “Frozen Rotor and Sliding Mesh Models Applied to the 3D Simulation of the Francis-99 Tokke Turbine with Code_Saturne,” J. Phys. Conf. Ser., vol. 755, no. 1, 2017.

[10] ANSYS, Inc, “Ansys Fluent Theory Guide, Release 2020 R1”, January 2020, Southpointe 2600 ANSYS Drive, Canonsburg, PA 15317.

[11] H K Versteeg and W Malalasekera, “An Introduction to Computational Fluid Dynamics-THE FINITE VOLUME METHOD”, Second Edition, ISBN: 978-0-13-127498-3, Pearson Education Limited, 2007